Isolating the sources of widespread physiological fluctuations in functional near-infrared spectroscopy signals

Yunjie Tong
Lia Maria Hocke
Blaise deB. Frederick

Isolating the sources of widespread physiological fluctuations in functional near-infrared spectroscopy signals

Yunjie Tong,[a,b] Lia Maria Hocke,[a,c] and Blaise deB. Frederick[a,b]
[a]McLean Hospital, Brain Imaging Center, 115 Mill Street, Belmont, Massachusetts 02478
[b]Harvard University Medical School, Department of Psychiatry, Boston, Massachusetts 02115
[c]University of Maastricht, Department of Psychology, Maastricht, The Netherlands

Abstract. Physiological fluctuations at low frequency (<0.1 Hz) are prominent in functional near-infrared spectroscopy (fNIRS) measurements in both resting state and functional task studies. In this study, we used the high spatial resolution and full brain coverage of functional magnetic resonance imaging (fMRI) to understand the origins and commonalities of these fluctuations. Specifically, we applied a newly developed method, regressor interpolation at progressive time delays, to analyze concurrently recorded fNIRS and fMRI data acquired both in a resting state study and in a finger tapping study. The method calculates the voxelwise correlations between blood oxygen level dependent (BOLD) fMRI and fNIRS signals with different time shifts and localizes the areas in the brain that highly correlate with the fNIRS signal recorded at the surface of the head. The results show the wide spatial distribution of this physiological fluctuation in BOLD data, both in task and resting states. The brain areas that are highly correlated with global physiological fluctuations observed by fNIRS have a pattern that resembles the venous system of the brain, indicating the blood fluctuation from veins on the brain surface might strongly contribute to the overall fNIRS signal. © *2011 Society of Photo-Optical Instrumentation Engineers (SPIE).* [DOI: 10.1117/1.3638128]

Keywords: functional near-infrared spectroscopy; resting state network; physiological fluctuation; functional connectivity.

Paper 11234R received May 11, 2011; revised manuscript received Aug. 4, 2011; accepted for publication Aug. 22, 2011; published online Oct. 14, 2011.

1 Introduction

Functional near-infrared spectroscopy (fNIRS) has become an increasingly common imaging technique due to its high temporal resolution, relative motion insensitivity, and cost-efficiency. However, in contrast to direct measurements of neuronal activity such as electroencephalography, fNIRS is an indirect measurement of brain function. It is sensitive to the hemodynamic changes caused by neuronal activity, but also by physiological processes, such as heartbeat, respiration, and low frequency oscillations.[1] Concentration changes in both oxy- ($\Delta[HbO]$) and deoxygenated hemoglobin ($\Delta[Hb]$) can be calculated with fNIRS.

Regional brain activations have been detected by fNIRS during functional tasks. These brain areas include: 1. the motor cortex activated by motor tasks like finger tapping,[2] 2. occipital cortex for visual tasks (reversing checkerboard),[3,4] 3. Broca's or Wernicke's area during auditory stimulation,[5,6] and 4. frontal cortex during cognitive tasks.[7–10] In the task periods, increases of $\Delta[HbO]$ accompanied by decreases in $\Delta[Hb]$ are commonly observed in the fNIRS signal, which can be explained by the Balloon model.[11] The model states that a higher metabolic rate evoked by brain activation causes an increase in regional blood flow in the capillary bed, resulting in an oxygenated blood flush into the activated brain region (increase in $\Delta[HbO]$) and dilution of local [Hb] (decrease in $\Delta[Hb]$). fNIRS measures brain activity by capturing the blood changes in the capillary bed caused

by brain function. However, in order to reach the capillary bed on the surface of the cerebral cortex, near-infrared light must traverse intervening compartments. The contributions of these layers, especially extra-cerebral ones (skin, skull), have been the focus of many studies.

Various studies have found significant contribution of the extracerebral layers to the overall fNIRS signal. Monte Carlo studies based on magnetic resonance imaging (MRI) generated 3D head models[12] suggest that the signals from the superficial layers affect fNIRS detection and become the dominant signal in short source-detector pairs [0.2 to 0.4 cm]. Concurrent fNIRS and transcranial laser Doppler studies of the human brain found high correlations between the signal derived from fNIRS and the laser Doppler skin blood flow, which implies a substantive contribution of the blood in the skin to the overall fNIRS signal.[13,14] Further support is provided by McCormick et al.[15] They separately injected indocyanine dye into the external and internal carotid arteries and observed signal changes of similar magnitude with both short and long source-detector pairs of fNIRS probes in the first case (external carotid artery injection), whereas only the signal from the long source-detector pair showed meaningful changes in the second case (internal carotid artery injection). Young et al.[16] demonstrated similar effects of the superficial layers by comparing the fNIRS signals while consecutively removing skin, skull, and dura under the detector or source during surgery. In summary, all these studies suggest that the surface signals are present in the fNIRS signal and that this contribution becomes more pronounced when the source-detector distance becomes smaller [<1 cm].

Address all correspondence to: Yunjie Tong, McLean Hospital, Brain Imaging Center, 115 Mill Street, Belmont, MA 02478; Tel: 617-855-3620; Fax: 617-855-3879; E-mail: ytong@mclean.harvard.edu.

Functional MRI (fMRI) is the most popular imaging tool to study brain functions due to its accuracy and noninvasiveness. Like fNIRS, fMRI indirectly measures neuronal activation through hemodynamic changes. Blood oxygen level dependent (BOLD) contrast causes the change of the fMRI signal intensity with changing local blood oxygenation and volume. Unlike fNIRS, fMRI offers much higher spatial resolution (2 to 3 mm versus 1 to 2 cm) and, more importantly, the ability to image the whole brain. These features make fMRI an excellent tool to study the sources of fNIRS signals. Concurrent fMRI and fNIRS studies have been conducted in order to compare the temporal trace of fNIRS signal and BOLD fMRI during functional tasks.[10,17] They found that spatially task-related regions of activation detected by fNIRS overlap with that of fMRI and within these regions, the temporal traces of the fNIRS signal (Δ[HbO] and Δ[Hb]) are highly correlated with that of BOLD fMRI. Those findings support the conclusion that the fNIRS signal does sample the activated capillary bed during functional tasks. However, these studies cannot thoroughly answer the question of the relative contribution to the fNIRS signal from the capillary bed versus the intervening layers for two reasons. The first reason is that most of these studies were done in functional tasks and are preprocessed to emphasize the task response at the expense of other signals. The second reason is that the regions of interest (ROI) studied in detail were confined to the corresponding activated region directly underneath the fNIRS probes. fNIRS data collected from the resting state, as well as the data from those probe locations remote from the activated area in the functional task, have rarely been studied in this way. The voxelwise correlation between fNIRS signal and BOLD fMRI throughout the whole brain have revealed some unexpected sources or features of the fNIRS signal.[18]

In this paper, we would like to extend these concurrent fMRI and fNIRS studies in order to understand the source of the fNIRS signal in the resting state and functional studies. We would utilize a method called regressor interpolation at progressive time delays (RIPTiDe)[19] in which fNIRS signals with various time shifts are utilized as regressors in an fMRI analysis, employing the general linear model (GLM). The method considers the temporal relationship between the signals in both modalities and correlates the BOLD signals from the whole brain with the fNIRS signal at various time shifts.

The RIPTiDe method has been applied to both resting state and functional studies, and demonstrates that, in addition to neuronal activity, fNIRS captures a great deal of the signal arising from global circulatory variations in many fNIRS channels. This global signal is highly correlated with the BOLD signal changes seen in the cerebrovascular system (especially large vessels), suggesting that a significant portion of the fNIRS signal reflects hemodynamic variations in the veins at the surface of the cortex.

2 Methods

2.1 Protocols and Instrumentation

To understand the source of fNIRS signal both during a resting state and task-related activation, we revisited two previously conducted concurrent fMRI/fNIRS studies, one of resting state activity and the other of motor response to a block finger tapping task. The details of the instrumentation and protocol have been previously described[17,18] (and are summarized in the Appendix).

Both acquisition protocols were approved by the McLean Hospital Institutional Review Board.

2.1.1 Concurrent resting state study

A concurrent fNIRS and fMRI resting state study was conducted on six healthy volunteers (four male and two female, aged 28.0 ± 4 years). A MRI-compatible fNIRS probe was placed on the right side of the prefrontal area of each subject (roughly between Fp1 and F7 according to the 10–20 system) to collect fNIRS data while he/she was scanned by a Siemens TIM Trio 3T scanner (Siemens Medical Systems, Malvern, Pennsylvania). The probe was designed to collect data from short and long source-detector pairs (1.0, 3.0 cm) at prefrontal cortex, where a well-known resting state network exists [Fig. 1(a)]. The total scan time was about 6 min and 30 s with 1.5 s repetition time (TR). The acquisition rate of fNIRS was 12.5 Hz. The fNIRS probe had three detector fibers and two source fibers with source-detector distances at 1 or 3 cm [Fig. 1(a)].

2.1.2 Concurrent finger tapping study

A block design finger tapping task was performed by a healthy subject (male, aged 30 years). The task included six periods of right-hand tapping alternated with rest periods (20 s tapping and 20 s rest). The MRI-compatible fNIRS helmet was worn by the subject during the experiment. The helmet consisted of four detectors and 16 sources arranged in a configuration that covered both hemispheres [Fig. 1(b)]. The acquisition rate of fNIRS was 6.25 Hz, while the TR was 2.02 s.

2.2 Functional Near-Infrared Spectroscopy and Functional Magnetic Resonance Imaging Data Analysis

In order to localize the source of fNIRS signal, we applied a newly-developed method (RIPTiDe) based on GLM to analyze both fNIRS and BOLD fMRI data together.[19] In brief, this method treats the temporally evolving blood related signal detected by both modalities as dynamic and progressive signals. Therefore, it uses the fNIRS signal and its temporal shifts (in both directions) as regressors into the voxelwise correlation with BOLD fMRI. The combined high-correlation map derived from this method includes all of the voxels that highly correlate with the fNIRS signal over a range of time lags. These voxels can be used to identify sources of fNIRS signals in the brain. All fMRI data processing was performed using FEAT, as part of the FSL analysis package (FMRIB Expert Analysis Tool, v5.98, http://www.fmrib.ox.ac.uk/fsl, Oxford University, United Kingdom).[20]

2.2.1 Resting state data analysis

In the case of resting state studies, four steps were required: 1. raw fNIRS time courses (690 and 830 nm data) were converted into two time courses representing Δ[HbO] and Δ[Hb] according to the differential path length factor method[21] using Matlab (The Mathworks, Natick, Massachusetts); 2. the time courses of Δ[HbO] from C1 (due to its high SNR for all subjects) and its temporally shifted versions (61: -7.2 to $+7.2$ s with steps of 0.24 s) were then anti-aliased and down-sampled to
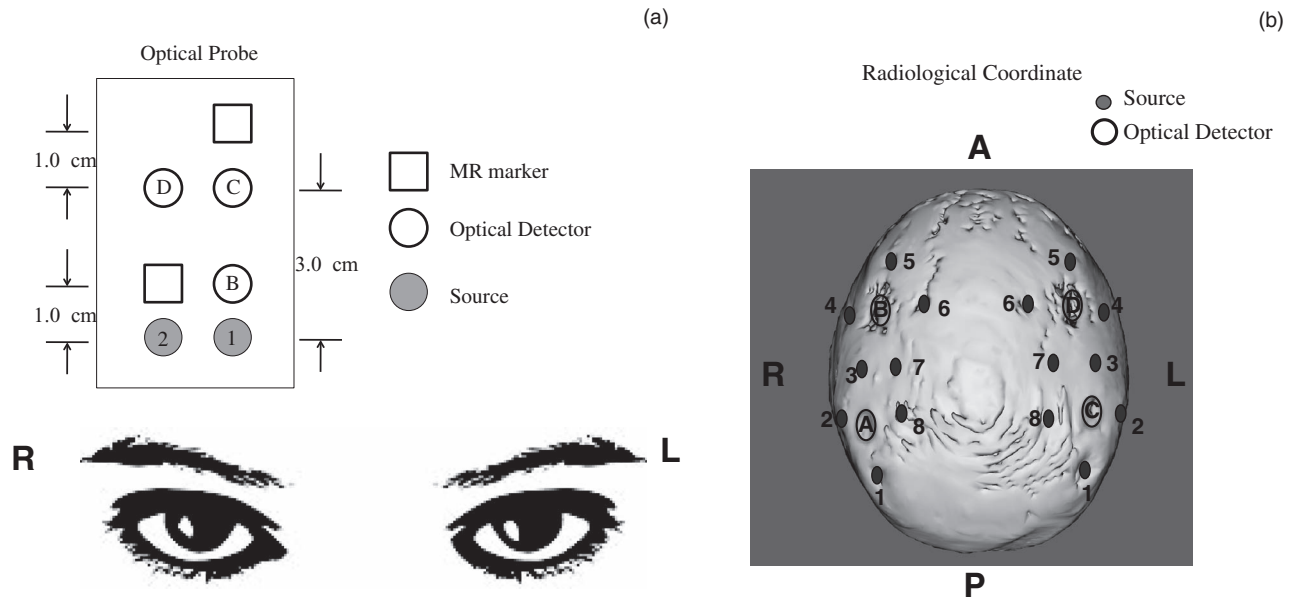
Fig. 1 Schematic diagrams of the optical probes and their placement in the (a) resting state and (b) finger tapping studies.

the fMRI acquisition frequency of 0.67 Hz (1/1.5 s), which had 260 data points; 3. each down-sampled time course was used as a regressor in fMRI data analysis, a total of 61 analyses were performed; and 4. the resulting 61 z-statistic maps were combined and the maximum z value was chosen for each voxel. The final maximum z-statistic map would include all of the voxels that had high correlation with fNIRS at certain time points.

2.2.2 Finger tapping experiment and data analysis

In order to study the contralateral and ipsilateral brain activation under the finger tapping task, the NIRS probe was designed to have the maximal coverage of motor cortex areas on both sides [Fig. 1(b)]. Both NIRS and fMRI data were simultaneously collected. A similar RIPTiDe procedure was applied on the finger tapping data with the following modifications: 1. The time course of $\Delta[HbO]$ and its time-shifted versions (21 time shifts: -2.4 to $+2.4$ s with steps of 0.24 s) from each source-detector pair were used as regressors in the analysis. In total, 21 analyses were performed for each source-detector pair; 2. In order to separate the neuronal motor activation from the physiological signal in fNIRS and BOLD fMRI data, the block diagram of the finger tapping periods was convolved with the hemodynamic delay function. The convolved timecourse and its derivative were utilized as the first two regressors in the BOLD fMRI analysis, followed by the delayed fNIRS regressor. The derivative is included to compensate for variations in the hemodynamic response and slice timing. In this case, we were interested in the localization of the source of the physiological signal that overlays the neuronal signal in fNIRS. By using the task timecourse as well as the data from fNIRS as the regressors, the convolved finger tapping timecourse and its derivative were treated as confounds to regress out any task-related portion of the fNIRS regressor, leaving the corresponding z-statistic maps of the fNIRS regressor to show only the significant response to the physiological signal. Figure 2 shows three regressors for one particular channel (C3) directly over the activated area as an example:

1. the finger tapping task (boxcar function) convolved with the hemodynamic function (double gamma function offered by the FSL package), 2. the temporal derivative, and 3. the resampled time traces of $\Delta[HbO]$ for C3.

3 Results

3.1 Resting State Result

3.1.1 Temporal traces

Figure 3 shows the resampled time traces of $\Delta[HbO]$ and $\Delta[Hb]$ measured at C1 and B1 on the foreheads of six subjects in the resting state studies. The resampling was required so that the fNIRS data could be used as regressors in the GLM analysis of the fMRI data. The anti-aliasing filter used in resampling applies a low pass filter (low pass $= 0.3$ Hz due to TR $= 1.5$ s).[18]
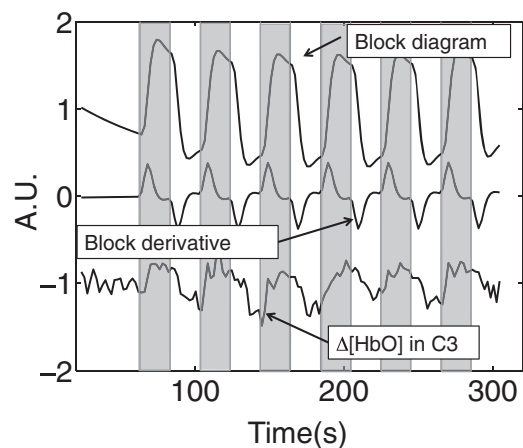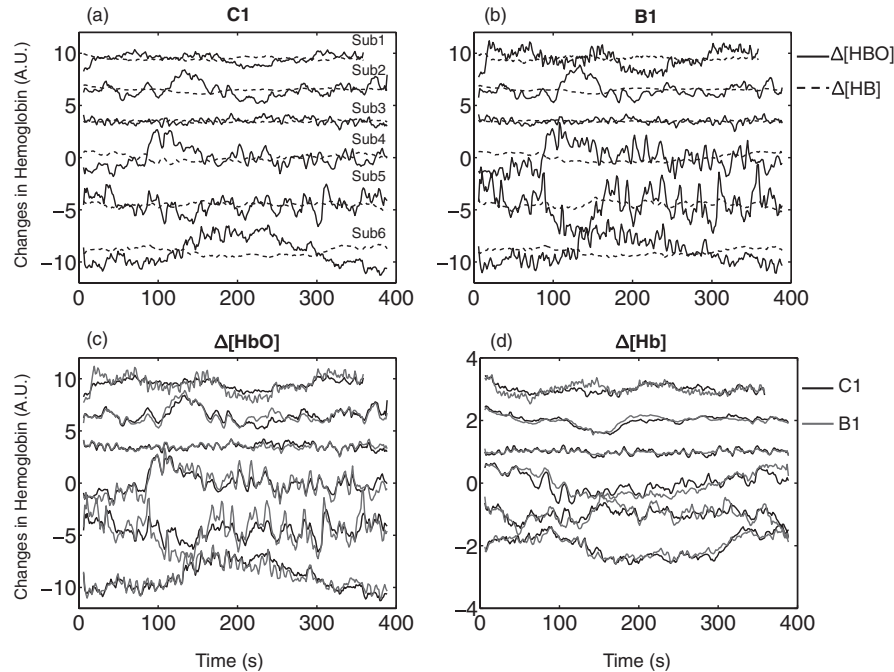

Fig. 2 Three regressors used in the analysis of the fMRI data obtained during a finger tapping task: 1. block diagram; 2. derivative of the block diagram; 3. resampled temporal trace of the $\Delta[HbO]$ from C3. Shaded areas indicate the tapping periods.

Fig. 3 Resampled temporal trace of the Δ[HbO] (solid black line) and Δ[Hb] (dotted black line) obtained during resting state from six subjects calculated from (a) C1 and (b) B1. To demonstrate the similarities between time traces of Δ[HbO] and Δ[Hb] measured in C1 and B1 for all subjects, (c) resampled temporal traces of the Δ[HbO] in B1 (gray) and C1 (black) were plotted for every subject, while in (d) resampled temporal traces of the Δ[Hb] in B1 and C1 were plotted.

Therefore, the heart beat signal is not visible in Fig. 3. Prominent features of the data are: 1. the Δ[HbO] signal is much bigger than that of Δ[Hb] as seen in Figs. 3(a) and 3(b), which is probably due to the high oxygenation of the blood throughout and 2. the phase of Δ[HbO] is not always 180 deg (anticorrelated) from that of Δ[Hb]. In fNIRS studies, a 180 deg phase difference between Δ[HbO] and Δ[Hb] obtained by fNIRS is commonly observed in the activated brain areas. However, the relationship between Δ[HbO] and Δ[Hb] in fNIRS resting state studies is not fully understood;[22] and 3. the Δ[HbO] measured from B1 (1 cm separation) in the same subject is highly correlated [as seen in Figs. 3(c) and 3(d)] with that from C1 (3 cm separation). The same is true for the Δ[Hb]. The average correlation coefficients are 0.82 and 0.80, respectively. This indicates that a significant proportion of the fNIRS signal recorded by both source-detector pairs (which are collinear but with different distances) is the same, which in turn means that either the source of most of the signal is within the range of both probes or the source of B1, which is at a shallow region and source of C1, which is at a deep region are highly correlated.

3.1.2 Spatial distribution

In order to better locate the source of the fNIRS signal (in C1 and B1), we conducted voxelwise correlation between the fNIRS signals and the BOLD fMRI using RIPTiDe.[19] Because Δ[HbO] has a much higher signal to noise ratio (SNR), and is demonstrated to be highly correlated with cerebral blood flow,[23] the results of using Δ[HbO] were the focus of the discussion. Figure 4 depicts the maximum z-statistic results of six subjects and the average of all subjects using Δ[HbO] from C1 [Fig. 4(a)] and Δ[HbO] from B1 [Fig. 4(b)]. The coronal (in the middle

panel) and axial (in the right panel) views of Figs. 4(a) and 4(b) were chosen to show the prefrontal area underneath the probe (the markers of the probe is visible in both graphs). In the result corresponding to C1 [Fig. 4(a)], the voxels underneath the probe were highly correlated with the fNIRS signal as expected. However, the activation patterns are global and symmetrical throughout the brain (the probe was on the right side only). The highest correlation was present in the voxels resembling the superior sagittal sinus, the inferior sagittal sinus, and straight sinus as displayed in the left panels of Fig. 4(a). Detailed discussion and graphs on the similarities of the correlation patterns of the subjects and their venous system (mainly on the surface of the cortex) were presented in our previous work,[18] in which the same resting state data was analyzed. In short, a 3D-rendered image of all of the activated voxels was similar to the phase contrast image (MRI technique to map the blood vessel only) and the passing of the activated voxels throughout the brain followed the same passage of the cerebral blood flow and matched the time of blood circulation. These findings indicate that part of the Δ[HbO] signals obtained by fNIRS probes (C1) might reflect the changes in the vein and venules on the surface of the brain. The fact that the brain area underneath the fNIRS probe and its contralateral equivalent were prominently visible in Fig. 4, implies that the neuronal signal (e.g., resting state network) may also be present in the fNIRS data. The results corresponding to B1 [Fig. 4(b)] are, to a large extent, similar to the ones shown in Fig. 4(a), as the symmetrical venous system. This is not surprising regarding the similarities between Δ[HbO] from C1 and B1 [seen in Fig. 3(c)]. However, for most of the subjects, smaller regions of activation underneath the probe were observed for B1 in Fig. 4(b), which is even more obvious in the averaged results, shown at the bottom of Fig. 4. To further quantitatively assess
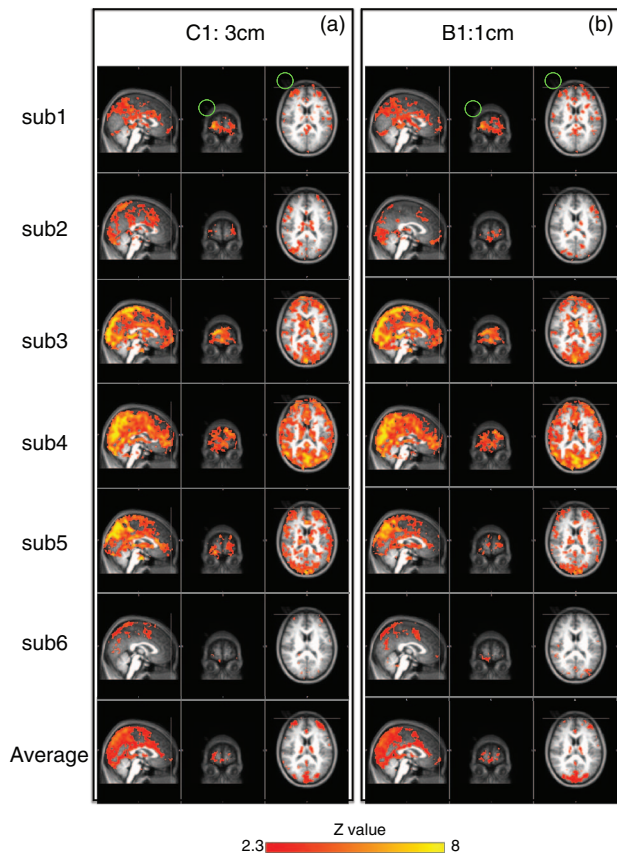
Fig. 4 Maximum z-statistic maps for six subjects in resting state studies were obtained by employing the RIPTiDe for Δ[HbO] from (a) C1 and (b) B1. The z-statistic maps were registered onto the averaged anatomical head images of the subjects. The averaged z-statistic maps for all subjects are shown in the bottom. The markers of the fNIRS probe can be seen in the green circles.

the difference in the activated areas (obtained from B1 and C1), we defined a ROI (on the averaged head of six subjects) underneath the probe that covers a big area from the surface of the cortex to 2.5 to 3.0 cm deep into the brain [Fig. 5(a)]. All of the activated voxels ($z > 2.3$) observed by B1 and C1 within this ROI were counted for each subject. The ratios (number of voxels from B1/C1) were calculated and showed in Fig. 5(b). From Fig. 5(b), we can see that only subject 4 has the ratio bigger than 1 (1.11 to be exact), indicating that a slightly bigger area
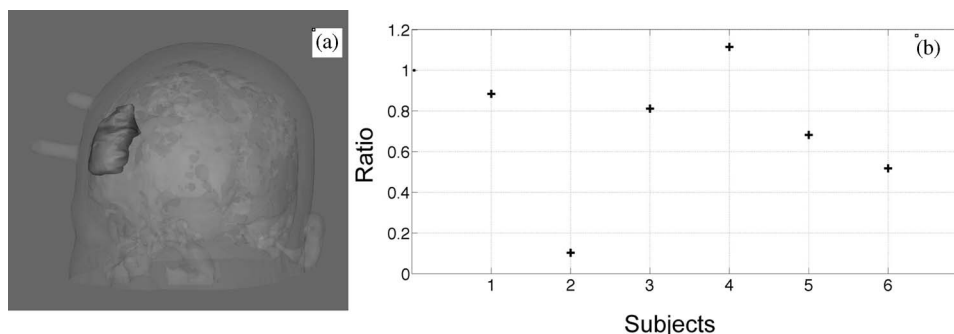
was observed for B1. For the rest of the five subjects, the ratios are smaller than 1 (ranging from 0.10 to 0.88), which confirmed that the smaller regions of activation underneath the probe were observed for B1. This indicates that most likely the sensitivity of B1 is lower in the cortex than that of C1, but it may nevertheless reach the surface veins.

3.2 Finger Tapping Result

3.2.1 Temporal correlation

A detailed analysis of the neuronal response to finger tapping in fMRI and fNIRS can be found in our previous work.[17] In this study, we will primarily focus on the physiological signal detected by fNIRS as opposed to the neuronal activity. Figure 6 shows the time traces of Δ[HbO] and Δ[Hb] for each channel surrounding four detectors. First, task activation was detected in C3 and C7, which were located over the motor cortex contralateral to the tapping hand. On the ipsilateral side, task-related deactivations were observed in A3 and A7 with negative z-values ($z = -4.4$ and -3.7 obtained from the correlation with task regressor). The reason why the finger tapping task evoked "activation" and "deactivation" on the contralateral and ipsilateral side of the brain is unclear and more subjects are needed to confirm the phenomenon. However, even in these task-related channels (C3, C7, A3, and A7), the physiological signal was nevertheless visible on top of the activation/deactivation patterns. In the other channels where task activation was not obviously visible, the physiological signal became the dominant signal. To further understand the internal relationship between the physiological signal detected by all of the channels, a high pass filter was applied to all 20 channels that are shown in Fig. 6, with low cutoff frequency at 0.025 Hz to filter out the neuronal effects of the finger tapping task (1/40 s = 0.025 Hz). The resulting time traces of Δ[HbO] and Δ[Hb] are shown in Figs. 7(a) and 7(c), respectively. The correlation coefficients among these channels are illustrated as tables in Figs. 7(b) and 7(d). Figure 7(a) shows that the temporal courses of Δ[HbO] from A1 to D7 (except A3 and A7) are highly correlated with each other despite their distributed (spatial) locations. This is further demonstrated by the correlation coefficient table in Fig. 7(b) in which the average correlation coefficient (except A3 and A7) is 0.69. This global correlation implies a strong underlying physiological fluctuation that affects most channels. The temporal traces of Δ[HbO] in A3 and A7 are correlated to each other with a correlation with
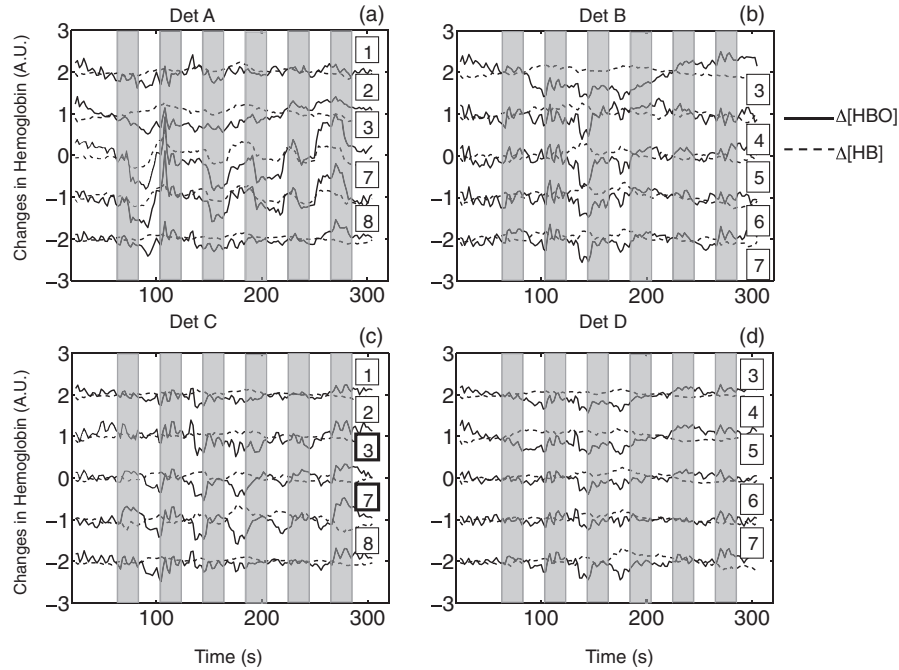

Fig. 5 (a) 3D rendered average head with ROI (gray blob) chosen underneath the NIRS probe. (b) Ratios between activated voxels (within the ROI) observed by B1 and that by C1 for each subject.

Fig. 6 Resampled temporal traces of Δ[HbO] (solid line) and Δ[Hb] (dotted line) obtained in (a) finger tapping task by detector A and its surrounding five sources (indicated by the numbers next to the temporal traces), (b) detector B, (c) detector C, and (d) detector D. Shaded areas indicate the tapping periods.
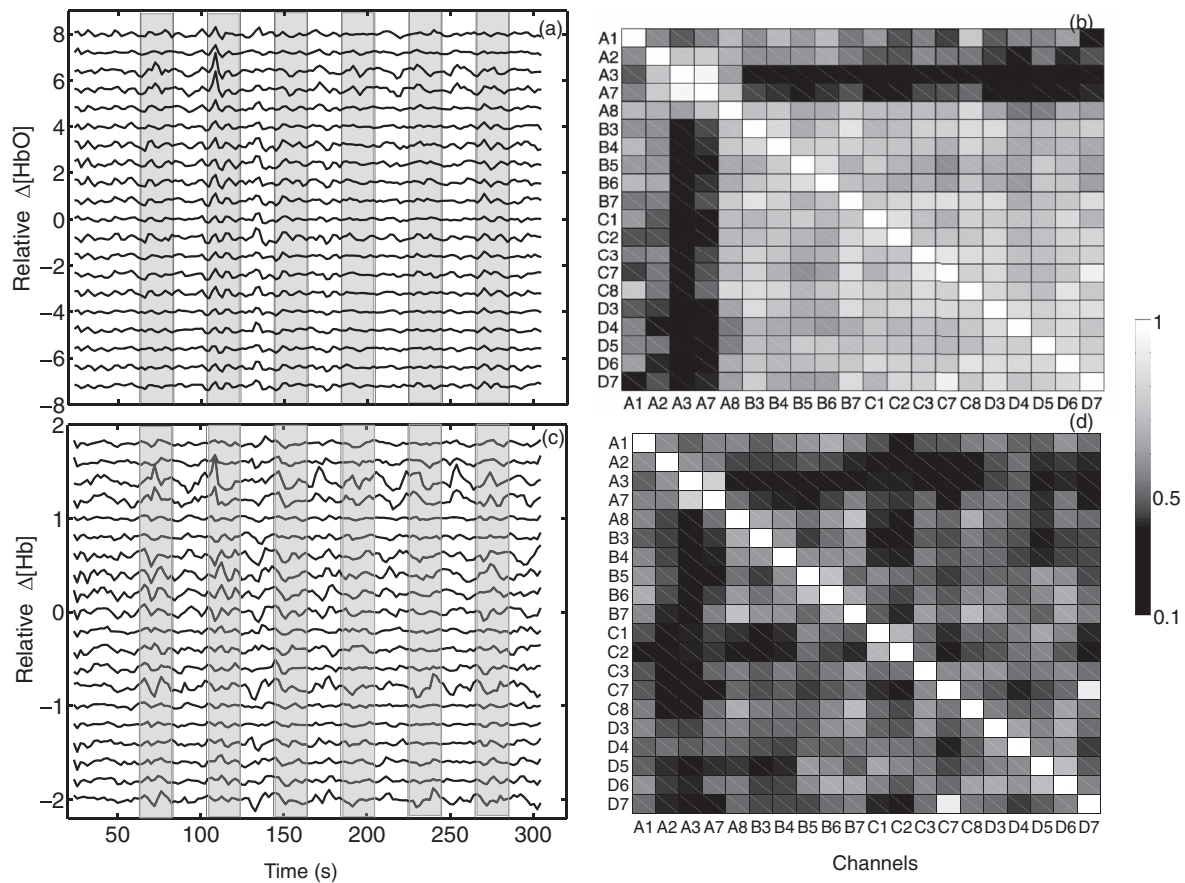
Fig. 7 High pass filtered resampled temporal traces of (a) Δ[HbO] and (c) Δ[Hb] from all the channels in the finger tapping task. The correlation coefficient table of temporal traces of (b) Δ[HbO] and (d) Δ[Hb]. Shaded areas indicate the tapping periods.
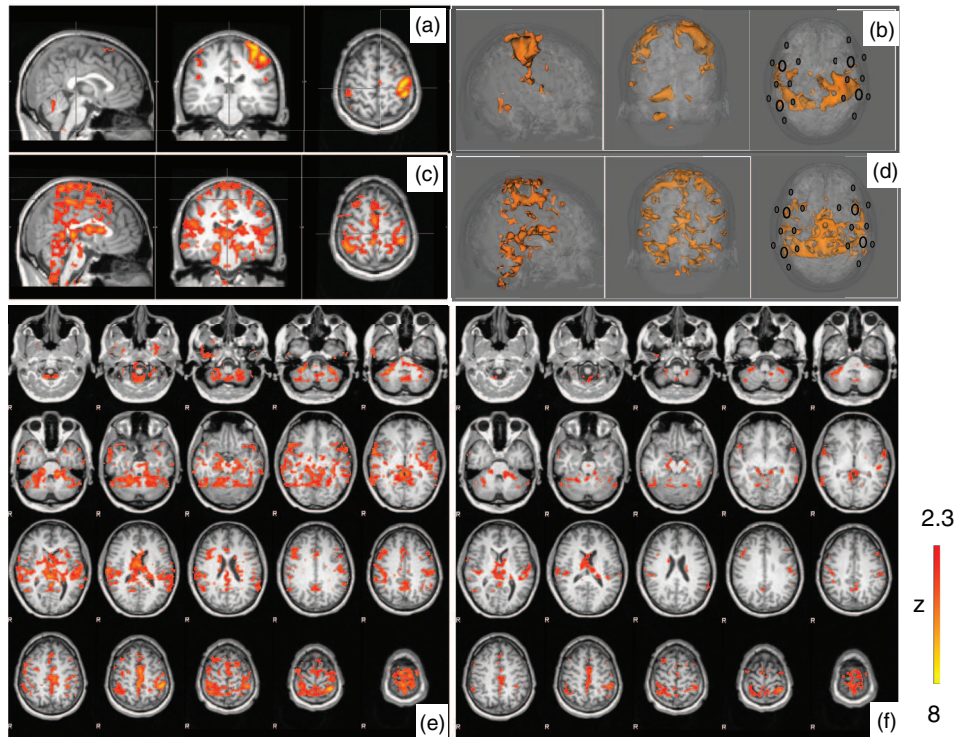
Fig. 8 z-statistic maps of the finger tapping task block diagram registered on (a) the subject's anatomical head and (b) its 3D rendered image with marked fNIRS probe. The maximum z-statistic maps obtained by RIPTiDe corresponding to the physiological fluctuation of C3 registered (c) on the subject's anatomical head and (e) its axial images. (d) 3D rendered images of the averaged maximum z-statistic maps of 20 channels (corresponding to the physiological fluctuation) and (f) their axial images.

coefficient as high as 0.93. Figure 7(c) displays the timecourses of Δ[Hb] from A1 to D7. Unlike Δ[HbO], in which the global correlation was observed, the location of the highly correlated channels of the Δ[Hb] are more (spatially) clustered. For example, high correlation was observed in the following groups: 1. A3 and A7; 2. B4, B5, B6, B7, and C1; and 3. C7 and D7. The average correlation coefficient is only 0.37.

3.2.2 Spatial location

In order to localize the global signal observed in almost every channel [Fig. 7(a)], we applied the modified RIPTiDe for each channel as described in Sec. 2. The depiction of the Δ[HbO] from channel C3 (in Fig. 2) was chosen to demonstrate that when used as a regressor in conjunction with the task regressor, the portion highly correlated with the finger tapping signal was essentially removed from the fNIRS regressor, allowing separate detection of the effect of the task and the physiological signal superimposed on the task response (removing the correlated portion of the two regressors). Figures 8(a), 8(c), and 8(e) show the corresponding z-statistic results of channel C3 in the brain areas activated by the task in Fig. 8(a) and the brain areas highly correlated with the physiological signal of fNIRS in Fig. 8(c) and their axial slices in Fig. 8(e). The corresponding averaged z-statistic results from all 20 channels were calculated and overlayed onto the structure brain of the subject and rendered into 3D images depicted in Figs. 8(b) and 8(d). The axial slices of the averaged results are also illustrated in Fig. 8(f).

The activation of the finger tapping task was clearly observed in both Figs. 8(a) and 8(b) as expected. More interestingly, the voxels correlated with the global physiological fluctuations, shown in Figs. 8(c)–8(f), are symmetrically spreading throughout the brain as visible in Fig. 4. Since we did not perform the whole head fMRI scan for the subject during the finger tapping task, only the middle portion of the brain is depicted in Figs. 8(c)–8(f). Nevertheless, the results show that areas that are highly correlated with the physiological signal seem to overlay the cerebrovascular system, especially the veins and venules as discussed in Sec. 3.1.2 of the spatial distribution of the resting state. This is further supported by the dynamic pattern of physiological activation generated by time-shifted NIRS regressors that follows the course of the circulating blood (data not shown).

4 Discussion

4.1 Likely Location of the Source of the Functional Near-Infrared Spectroscopy Signal

fNIRS has been proven to be sensitive to the area resembling a banana shape under the source-detector pair.[24] Thus, many concurrent fMRI and fNIRS studies focused on the area directly underneath the fNIRS probe.[17,25] In this study, we extended our analysis to the whole brain using a new analyzing method (RIPTiDe) for the fNIRS signal and BOLD fMRI together. The method is able to localize the voxels correlating with the fNIRS signal at different time lags. The results depicted in Figs. 4 and 8(c)–8(f), show that the voxels, which highly correlate with

Δ[HbO] measured by fNIRS, are found in the regions where blood vessels and especially the surface veins reside. This indicates that one likely location for the source of the fNIRS signal may be the veins on the surface of the cortex. This argument is further supported by three observations. First, anatomically, compared to arteries that deliver the blood through the midbrain, the massive and symmetrical distributed veins cover the surface of the cortex,[26] collect the blood, and drain it through larger veins, such as the superior sagittal sinus. There are arterioles on the surface of the cortex as well, however, they are much smaller. Because of the high density of the veins over the surface and the high concentration of blood in these veins, any blood fluctuation in them would change the absorption of the photons and make it detectable by the fNIRS probe. This physiological signal could become dominant if no other signal from the surrounding capillary bed evoked by brain function surpasses it. Second, the amount of blood in the extracerebral layers is small compared to that at the surface of the cortex. This is even more true when the blood is further squeezed out of the skin by the pressure of the fNIRS probe. The third observation comes from our previous study,[18] which demonstrated that the blood signal from the veins are highly correlated with each other. Therefore, the global signal observed in Fig. 7(a) is likely to be the signal derived from the veins detected by multiple fNIRS channels at largely distributed locations, but still highly correlated with each other. The other possible source of this physiological fluctuation comes from the surface layers of the brain (skin and skull) as discussed in the introduction. We were not able to calculate the reliable correlation between the BOLD signal from the surface layers and the signal from fNIRS due to the low SNR of the BOLD caused by limited blood presented in these layers. Our results do not contradict this argument, but rather point out that if this argument is true, the blood fluctuations from the surface layers have to temporally correlate (with/without time delays) with that of the veins on the cortex. In summary, our results demonstrate the pervasiveness of this physiological blood fluctuation in the fNIRS signal.

This global physiological fluctuation was detected by fNIRS in both resting state studies (Fig. 4) as well as functional studies [Fig. 8(c)–8(f)]. In both cases, the fNIRS signal is likely to be the sum of the neuronal activation of the brain function (mainly from the capillary bed) and the physiological fluctuation. Which signal dominates the overall fNIRS signal, the neuronal activation (resting state or task related signal) or the physiological fluctuations (vein signals), depends on the location of the fNIRS probe and the strength of the neuronal activation (from the capillary bed). In Fig. 6(c), Δ[HbO] from C3 and C7 clearly shows the neuronal activation as the dominant signal due to the placement of these source detector pairs directly above the activation sites [Fig. 1(b)] and the strong signal caused by the finger tapping task. In some other channels, such as C1, C2, and C8, the physiological fluctuations are dominant due to the location of the probes (off the site of activation).

In resting state data, we demonstrate that part of the fNIRS signal is due to this global physiological fluctuation. Since the brain function in the resting state is not as predictable as in the case of finger tapping, the neuronal activation pattern (commonly called "resting state network") is harder to isolate from the physiological fluctuations. Many efforts have been put into the fNIRS resting-state networks research to single this noise

out.[27–30] Among them, Mesquita et al.[28] averaged the time series over all fNIRS channels on the head to identify the global signal and later remove it, while White et al.[27] used the same procedure, but averaging the data collected only from the short source-detector distance pairs. Zhang et al.[30] used independent component analysis to separate the global noise from the signal. The contributions of our research is twofold. First, we associate this global fluctuations with the veins or venules on the surface of the cortex. As a consequence, this signal is symmetric and widely detectable by fNIRS. Second, we propose to use the RIP-TiDe method in order to remove this global dynamic fluctuation from the fNIRS data by dedicating a single confound source-detector pair to capture only the global blood signal (e.g., by placing the pair over the superior sagittal sinus).

4.2 Δ[HbO] and Δ[Hb]

In this study, the analyses were done using the Δ[HbO] calculated from fNIRS data. The reasons are threefold. First, Δ[HbO] has a much higher SNR than that of Δ[Hb], thus, using Δ[HbO] as a regressor can produce more reliable results. Second, utilizing an animal model, Hoshi et al. demonstrated that Δ[HbO] consistently correlated with rCBF, which is not the case in Δ[Hb],[23] thus, Δ[HbO] more accurately reflects the dynamics in the blood than Δ[Hb] does. Third, Δ[HbO] has been widely used in the resting state network analysis due to its high SNR,[30,31] therefore, understanding the source of Δ[HbO] could be beneficial to these studies.

Temporal traces of Δ[Hb] are also depicted in Figs. 3, 6, and 7. In resting state data (Fig. 3), most Δ[Hb] signals anticorrelate with Δ[HbO] from the same channel with no or small time lag (∼1.5 s). Anticorrelation was observed in four out of six subjects ranging from −0.67 to −0.91, whereas two subjects had very low correlations (<0.1). There have been a few studies on the correlations between Δ[HbO] and Δ[Hb] in resting state measurements.[32–34] Our data suggests that anticorrelation between the changes in the two hemoglobin species in the resting state indicate that fNIRS might measure the blood flow changes after all.

In the motor activation study, in the channels covering the brain area where finger tapping related activation was visible [C3 and C7 in Fig. 6(c)], Δ[Hb] was anticorrelated with Δ[HbO] as predicted. However, the relationship between Δ[Hb] and Δ[HbO] was not as straightforward in the study of the fluctuations superimposing the finger tapping related activities. This is demonstrated in Fig. 7(c) in which the high pass filter was applied on Δ[Hb] to remove the finger tapping related signals. The correlation coefficients between corresponding Δ[Hb] and Δ[HbO] pairs are ranging from +0.8 to −0.8. Among them, weak negative correlation and some positive correlations were observed only in A1, A2, A3, and A7 (with correlation coefficients as −0.16 0.16, 0.80, 0.48, respectively), the rest of the sixteen channels showed the negative correlations (with the mean correlation coefficient and its standard deviation as −0.62 ± 0.16). This result indicates that in most channels, even after removing the finger tapping related signals, anticorrelation exists between Δ[HbO] and Δ[Hb].

Cui et al.[35] explored the relationship between Δ[HbO] and Δ[Hb] in fNIRS studies and used positive correlations to identify the motion artifacts. However, in our study, the motion

parameters calculated by FSL could not explain the positive correlations we observed in channels A2, A3, and A7. Therefore, we argue that although motion artifacts generate positive correlations between Δ[HbO] and Δ[Hb], it seems not true that all of the positive correlations are due to motion artifacts.

Unlike the global correlation found in Δ[HbO] [Fig. 7(a) and 7(b)], the correlations in Δ[Hb] regionally happened as discussed in Sec. 3.2.1. This is supported by the research of Hoshi et al.[23,36] suggesting that the direction of Δ[Hb] would be locally decided by two opposite factors, namely venous blood oxygenation and blood volume.

4.3 Frequency of the Functional Near-Infrared Spectroscopy Signal

In our studies, fNIRS signal was downsampled to the acquisition frequencies of fMRI (1/1.5 and 1/2.02 s, respectively). The downsampling procedure acted as a low pass filter on the fNIRS data with cutoff frequencies around 0.3 and 0.25 Hz (determined by the TR). Therefore, the physiological signal from the heartbeat was removed from the fNIRS signal. Furthermore, in the FEAT analysis, a high pass filter of 0.01 Hz was applied to the regressors as well as to the BOLD fMRI signal in order to remove very low frequency oscillations mainly caused by instrumental noise. As a result, the analyzed signal spectrum ranged between 0.01 to 0.3/0.25 Hz. The signal of this range is of great interest in both BOLD fMRI and fNIRS, because it covers the signal frequency from most functional block design studies (e.g., finger tapping). Moreover, the signal of spontaneous low frequency oscillation (LFO), defined between 0.01 to 0.1 Hz, is a crucial factor in determining the resting state network.[37,38] Our previous work[18] implied that one major component of these LFOs originated outside of the brain and propagated along the cerebrovascular system. The present study indicates that this physiological LFO is prone to be detected by the fNIRS probes in both resting state and during functional tasks at multiple locations of the brain.

4.4 Short Distance versus Long Distance Functional Near-Infrared Spectroscopy Measurement

It has been suggested that by incorporating a source-detector pair with short distance (less than 1 cm), the signal mainly from the extracerebral layers can be sampled and later removed from the adjacent long source-detector probe that is supposed to pick up the signal from both the extracerebral as well as the intracerebral regions. The method is normally referred to as the subtraction (linear regression) method.[39,40] In our study of the resting state, we used both short (1 cm) and long distance (3 cm) probes on the same area [B1 and C1 in Fig. 1(a)]. Figures 3(c) and 3(d) compares the temporal traces of Δ[HbO] and Δ[Hb] detected by these two probes for all six subjects, where the high correlation between the corresponding time traces is prominent for all subjects. The same RIPTiDe analyses were applied using Δ[HbO] from both short and long source-detector pairs (B1 and C1) yielding similar results [Figs. 4(a) and 4(b)]. Thus, our data suggests another possible explanation, besides the surface layer contribution, namely that the signal detected by the fNIRS probe of short distance (1 cm) is influenced by the veins from the surface of the cortex as is that of

the long distance probe. The difference between the signal obtained from short and long source-detector pairs would be that the probe with long source-detector distance could, in addition to the vein signal, also sample the capillary bed surrounding the vein due to its extended depth of sensitivity. This is demonstrated by the difference in the results obtained by utilizing Δ[HbO] from C1 and B1 (as shown in Figs. 4 and 5). Smaller regions of activation underneath the probe were observed for B1, indicating that B1 has smaller depth of sensitivity. When the signal from the short source-detector pair was subtracted from that of the long source-detector pair, the vein signal (physiological) might have been mostly removed, leaving the signal of the capillary bed. Therefore, the subtraction method would also work.

The subtraction method was applied in our resting state study, however, due to the very limited fNIRS coverage (small probe) in the studies, it is not easy to interpret the results and more research has to be done concerning this issue.

5 Conclusion

In this study, a novel method called RIPTiDe was applied to the data concurrently collected by fNIRS and fMRI to explore the origins of the global fluctuations observed in fNIRS signal in both resting state and functional studies. The method was based on voxelwise correlation between the fNIRS signal (Δ[HbO]) and BOLD fMRI in order to identify the brain area highly correlatated with the fNIRS signal of certain time lags. Our results show high correlation between the synchronized blood fluctuation in the surface veins of the cortex and the fNIRS signal regardless of the location of the probes. This physiological fluctuation seems widely present, even dominating some fNIRS signals in the resting state, while superimposing neuronal activation signals in functional studies. Since this signal is related to global cerebral blood flow (not to neuronal activation) and is widely accessible by fNIRS, we argue that great caution is needed in fNIRS studies, especially in studies on resting state networks.

Appendix A: Functional Magnetic Resonance Imaging Acquisition

Both MR data from resting state and finger tapping were acquired on a Siemens TIM Trio 3T scanner (Siemens Medical Systems, Malvern, Pennsylvania) using a 12-channel phased array head matrix coil. In each resting state scan, a high-resolution anatomic image set was acquired for slice positioning and co-registration of the functional data [T1 weighted multiecho MP-RAGE3D,[41] resolution (RL, AP, SI) of $1.33 \times 1 \times 1$ mm, TI = 1100 ms, TR/TE1,TE2 = 2530/3.31,11.61 ms, more accurately (FOV) = $171 \times 256 \times 256$ mm, $128 \times 256 \times 256$ pixels, $2\times$ GRAPPA, total imaging time 4 min 32 s]. This was followed by the RS scans with identical parameters (two dummy shots, 260 time points, TR/TE = 1500/30 ms, flip angle 75 deg, matrix = 64×64 on a 220×220 mm FOV, 29 3.5 mm slices with 0.5 mm gap parallel to the AC-PC line extending down from the top of the brain, GRAPPA acceleration factor of 3). In the finger tapping scan, after localization and shimming, a series of fMRI images are acquired. Image parameters are as follows: gradient echo EPI, TE/TR = 30/2020 ms, 64×64 image

matrix, full k-space acquisition, FOV 220 × 220, 30 interleaved coronal slices (R/L readout), 3 mm thick, 0 mm gap, with the slice stack centered on the motor strip. A total of 120 time points are acquired after 12 dummy shots.

Appendix B: Functional Near-Infrared Spectroscopy Acquisition

In both resting state and finger tapping studies, NIRS data was collected by means of an MRI compatible fNIRS probe placed on each participant's head. The probe consisted of the collection and illumination of optical fibers. Each illumination fiber delivered light from two laser diodes emitting at wavelengths of 690 and 830 nm. The laser diodes and the optical detectors (photomultipliers tubes, Hamamatsu Photonics R928) were housed in a near-infrared tissue imager (Imagent, ISS, Inc., Champaign, Illinois), which was placed in the MRI control room. The optical probe and the Imagent instrument were connected by 10 m long optical fibers. The sampling rate of fNIRS data acquisition was 12.5 Hz in resting state sudies and 6.25 Hz in the finger tapping study. The exact locations of the probe and its source-detector pairs are known by the MR-visible markers or the imprints left by the fibers on the anotomical scans.

References

1. T. J. Huppert, S. G. Diamond, M. A. Franceschini, and D. A. Boas, "HomER: a review of time-series analysis methods for near-infrared spectroscopy of the brain," *Appl. Opt.* **48**(10), D280–D298 (2009).
2. M. A. Franceschini, V. Toronov, M. Filiaci, E. Gratton, and S. Fantini, "On-line optical imaging of the human brain with 160-ms temporal resolution," *Opt. Express* **6**(3), 49–57 (2000).
3. K. Takahashi, S. Ogata, Y. Atsumi, R. Yamamoto, S. Shiotsuka, A. Maki, Y. Yamashita, T. Yamamoto, H. Koizumi, H. Hirasawa, and M. Igawa, "Activation of the visual cortex imaged by 24-channel near-infrared spectroscopy," *J. Biomed. Opt.* **5**(1), 93–96 (2000).
4. B. W. Zeff, B. R. White, H. Dehghani, B. L. Schlaggar, and J. P. Culver, "Retinotopic mapping of adult human visual cortex with high-density diffuse optical tomography," *Proc. Natl. Acad. Sci. U.S.A.* **104**(29), 12169–12174 (2007).
5. P. Zaramella, F. Freato, A. Amigoni, S. Salvadori, P. Marangoni, A. Suppjei, B. Schiavo, and L. Chiandetti, "Brain auditory activation measured by near-infrared spectroscopy (NIRS) in neonates," *Pediatr. Res.* **49**(2), 213–219 (2001).
6. S. Chen, K. Sakatani, W. Lichty, P. Ning, S. Zhao, and H. Zuo, "Auditory-evoked cerebral oxygenation changes in hypoxic-ischemic encephalopathy of newborn infants monitored by near infrared spectroscopy," *Early Hum. Dev.* **67**(1–2), 113–121 (2002).
7. F. Tian, B. Chance, and H. Liu, "Investigation of the prefrontal cortex in response to duration-variable anagram tasks using functional near-infrared spectroscopy," *J. Biomed. Opt.* **14**(5), 054016 (2009).
8. G. Pfurtscheller, G. Bauernfeind, S. C. Wriessnegger, and C. Neuper, "Focal frontal (de)oxyhemoglobin responses during simple arithmetic," *Int. J. Psychophysiol* **76**(3), 186–192 (2010).
9. S. D. Power, T. H. Falk, and T. Chau, "Classification of prefrontal activity due to mental arithmetic and music imagery using hidden Markov models and frequency domain near-infrared spectroscopy," *J. Neural Eng.* **7**(2), 26002 (2010). notlisted
10. X. Cui, S. Bray, D. M. Bryant, G. H. Glover, and A. L. Reiss, "A quantitative comparison of NIRS and fMRI across multiple cognitive tasks," *Neuroimage* **54**(4), 2808–2821 (2011).
11. R. B. Buxton, E. C. Wong, and L. R. Frank, "Dynamics of blood flow and oxygenation changes during brain activation: the balloon model," *Magn. Reson. Med.* **39**(6), 855–864 (1998).
12. C. Mansouri, P. L'Huillier J, N. H. Kashou, and A. Humeau, "Depth sensitivity analysis of functional near-infrared spectroscopy measurement using three-dimensional Monte Carlo modelling-based magnetic resonance imaging," *Lasers Med. Sci.* **25**(3), 431–438 (2010).
13. S. L. Davis, P. J. Fadel, J. Cui, G. D. Thomas, and C. G. Crandall, "Skin blood flow influences near-infrared spectroscopy-derived measurements of tissue oxygenation during heat stress," *J. Appl. Physiol.* **100**(1), 221–224 (2006).
14. S. Kohno, I. Miyai, A. Seiyama, I. Oda, A. Ishikawa, S. Tsuneishi, T. Amita, and K. Shimizu, "Removal of the skin blood flow artifact in functional near-infrared spectroscopic imaging data through independent component analysis," *J. Biomed. Opt.* **12**(6), 062111 (2007).
15. P. W. McCormick, M. Stewart, G. Lewis, M. Dujovny, and J. I. Ausman, "Intracerebral penetration of infrared light. Technical note," *J. Neurosurg.* **76**(2), 315–318 (1992).
16. A. E. Young, T. J. Germon, N. J. Barnett, A. R. Manara, and R. J. Nelson, "Behaviour of near-infrared light in the adult human head: implications for clinical near-infrared spectroscopy," *Br. J. Anaesth.* **84**(1), 38–42 (2000).
17. A. Sassaroli, B. F. B. de, Y. Tong, P. F. Renshaw, and S. Fantini, "Spatially weighted BOLD signal for comparison of functional magnetic resonance imaging and near-infrared imaging of the brain," *Neuroimage* **33**(2), 505–514 (2006).
18. Y. Tong and B. D. Frederick, "Time lag dependent multimodal processing of concurrent fMRI and near-infrared spectroscopy (NIRS) data suggests a global circulatory origin for low-frequency oscillation signals in human brain," *Neuroimage* **53**(2), 553–564 (2010).
19. Y. Tong, P. R. Bergethon, and B. D. Frederick, "An improved method for mapping cerebrovascular reserve using concurrent fMRI and near infrared spectroscopy with Regressor Interpolation at Progressive Time Delays (RIPTiDe)," *Neuroimage* **56**(4), 2047–2057 (2011).
20. S. M. Smith, et al., "Advances in functional and structural MR image analysis and implementation as FSL," *Neuroimage* **23** Suppl 1, S208–S219 (2004).
21. S. J. Matcher, "Use of the water absorption spectrum to quantify tissue chromophore concentration changes in near-infrared spectroscopy," *Phys. Med. Biol.* **39**(1), 177–196 (1994).
22. F. Zheng, A. Sassaroli, and S. Fantini, "Phasor representation of oxy- and deoxyhemoglobin concentrations: what is the meaning of out-of-phase oscillations as measured by near-infrared spectroscopy?," *J. Biomed. Opt.* **15**(4), 040512 (2010).
23. Y. Hoshi, N. Kobayashi, and M. Tamura, "Interpretation of near-infrared spectroscopy signals: a study with a newly developed perfused rat brain model," *J. Appl. Physiol.* **90**(5), 1657–1662 (2001).
24. S. Feng, F. A. Zeng, and B. Chance, "Photon migration in the presence of a single defect: a perturbation analysis," *Appl. Opt.* **34**(19), 3826–3837 (1995).
25. T. J. Huppert, R. D. Hoge, S. G. Diamond, M. A. Franceschini, and D. A. Boas, "A temporal comparison of BOLD, ASL, and NIRS hemodynamic responses to motor stimuli in adult humans," *Neuroimage* **29**(2), 368–382 (2006).
26. M. Schuenke, E. Schulte, U. Schumacher, and L. Ross, *Head and Neuroanatomy*, Thieme, Stuttgart, New York (2010).
27. B. R. White, A. Z. Snyder, A. L. Cohen, S. E. Petersen, M. E. Raichle, B. L. Schlaggar, and J. P. Culver, "Resting-state functional connectivity in the human brain revealed with diffuse optical tomography," *Neuroimage* **47**(1), 148–156 (2009).
28. R. C. Mesquita, M. A. Franceschini, and D. A. Boas, "Resting state functional connectivity of the whole head with near-infrared spectroscopy," *Biomed. Opt. Express* **1**(1), 324–336 (2010).
29. H. Zhang, Y. J. Zhang, C. M. Lu, S. Y. Ma, Y. F. Zang, and C. Z. Zhu, "Functional connectivity as revealed by independent component analysis of resting-state fNIRS measurements," *Neuroimage* **51**(3), 1150–1161 (2010).
30. Y. J. Zhang, C. M. Lu, B. B. Biswal, Y. F. Zang, D. L. Peng, and C. Z. Zhu, "Detecting resting-state functional connectivity in the language system using functional near-infrared spectroscopy," *J. Biomed. Opt.* **15**(4), 047003 (2010).

31. H. Niu, C. M. Lu, C. Zhu, S. Khadka, F. Tian, Z. Lin, and H. Liu, "Resting-state functional connectivity assessed with two diffuse optical tomographic systems," *J. Biomed. Opt.* **16**(4), 046006 (2011).
32. H. Obrig, M. Neufang, R. Wenzel, M. Kohl, J. Steinbrink, K. Einhaupl, and A. Villringer, "Spontaneous low frequency oscillations of cerebral hemodynamics and metabolism in human adults," *Neuroimage* **12**(6), 623–639 (2000).
33. G. Taga, Y. Konishi, A. Maki, T. Tachibana, M. Fujiwara, and H. Koizumi, "Spontaneous oscillation of oxy- and deoxy- hemoglobin changes with a phase difference throughout the occipital cortex of newborn infants observed using non-invasive optical topography," *Neurosci. Lett.* **282**(1–2), 101–104 (2000).
34. M. Reinhard, E. Wehrle-Wieland, D. Grabiak, M. Roth, B. Guschlbauer, J. Timmer, C. Weiller, and A. Hetzel, "Oscillatory cerebral hemodynamics–the macro- vs. microvascular level," *J. Neurosci.* **250**(1–2), 103–109 (2006).
35. X. Cui, S. Bray, and A. L. Reiss, "Functional near infrared spectroscopy (NIRS) signal improvement based on negative correlation between oxygenated and deoxygenated hemoglobin dynamics," *Neuroimage* **49**(4), 3039–3046 (2010).
36. Y. Hoshi, "Functional near-infrared spectroscopy: current status and future prospects," *J. Biomed. Opt.* **12**(6), 062106 (2007).
37. D. P. Auer, "Spontaneous low-frequency blood oxygenation level-dependent fluctuations and functional connectivity analysis of the 'resting' brain," *Magn. Reson. Imaging* **26**(7), 1055–1064 (2008).
38. X. N. Zuo, A. Di Martino, C. Kelly, Z. E. Shehzad, D. G. Gee, D. F. Klein, F. X. Castellanos, B. B. Biswal, and M. P. Milham, "The oscillating brain: complex and reliable," *Neuroimage* **49**(2), 1432–1445 (2010).
39. R. Saager and A. Berger, "Measurement of layer-like hemodynamic trends in scalp and cortex: implications for physiological baseline suppression in functional near-infrared spectroscopy," *J. Biomed. Opt.* **13**(3), 034017 (2008).
40. L. Gagnon, K. Perdue, D. N. Greve, D. Goldenholz, G. Kaskhedikar, and D. A. Boas, "Improved recovery of the hemodynamic response in diffuse optical imaging using short optode separations and state-space modeling," *Neuroimage* **56**(3), 1362–1371 (2011).
41. A. J. van der Kouwe, T. Benner, D. H. Salat, and B. Fischl, "Brain morphometry with multiecho MPRAGE," *Neuroimage* **40**(2), 559–569 (2008).